HHS Public Access

Author manuscript

Pharm Res. Author manuscript; available in PMC 2016 August 01.

Published in final edited form as:

Pharm Res. 2015 August ; 32(8): 2690–2703. doi:10.1007/s11095-015-1653-y.

PTD-Modified ATTEMPTS for Enhanced Toxin-based Cancer Therapy: An *In Vivo* Proof-of-Concept Study

Meong Cheol Shin[a,b], **Jian Zhang**[c], **Kyoung Ah Min**[b], **Huining He**[a], **Allan E. David**[d], **Yongzhuo Huang**[e], and **Victor C. Yang**[a,b,f,*]

[a] Tianjin Key Laboratory on Technologies Enabling Development of Clinical Therapeutics and Diagnosis, School of Pharmacy, Tianjin Medical University, Tianjin 300070, China

[b] Department of Pharmaceutical Sciences, College of Pharmacy, University of Michigan, 428 Church St., Ann Arbor, MI 48109, USA

[c] Biomedical Polymers Laboratory, and Jiangsu Key Laboratory of Advanced Functional Polymer Design and Application, Department of Polymer Science and Engineering, College of Chemistry, Chemical Engineering and Materials Science, Soochow University, Suzhou 215123, China

[d] Department of Chemical Engineering, Auburn University, Auburn, AL 36849, USA

[e] Shanghai Institute of Materia Medica, Chinese Academy of Sciences, 501 Hai-ke Rd, Shanghai 201203, China

[f] Department of Molecular Medicine and Biopharmaceutical Sciences, Graduate School of Convergence Science and Technology, and College of Medicine or College of Pharmacy, Seoul National University, Seoul, 151-742, Republic of Korea

Abstract

Purpose—To investigate the feasibility of applying PTD-modified ATTEMPTS (Antibody Targeted Triggered Electrically Modified Prodrug-Type Strategy) for enhanced toxin therapy for the treatment of cancer.

Methods—A heparin-functionalized murine anti-CEA monoclonal antibody (mAb), T84.66-heparin (T84.66-Hep), was chemically synthesized and characterized for specific binding to CEA overexpressed cells. The T84.66-Hep was then applied to the PTD-modified ATTEMPTS approach and the crucial features of the drug delivery system (DDS), 'antibody targeting' and 'heparin/protamine-based prodrug', were evaluated *in vitro* to examine whether it could selective delivery a PTD-modified toxin, recombinant TAT-gelonin chimera (TAT-Gel), to CEA high expression cancer cells (LS174T). Furthermore, the feasibility of the drug delivery system (DDS) was assessed *in vivo* by biodistribution and efficacy studies using LS174T *s.c.* xenograft tumor bearing mice.

Results—T84.66-Hep displayed specific binding, but limited internalization (35% after 48 h incubation) to CEA high expression LS174T cells over low expression HCT116 cells. When

* Author to whom correspondence should be addressed: Victor C. Yang, Ph.D. Albert B Prescott Professor Department of Pharmaceutical Sciences The University of Michigan Ann Arbor, Michigan 48109-1065 Tel: 01-734-764-4273; Fax: 01-734-763-9772 vcyang@umich.edu.

mixed together with TAT-Gel, the T84.66-Hep formed a strong yet reversible complex. This complex formation provided an effective means of active tumor targeting of TAT-Gel, by 1) directing the TAT-Gel to CEA overexpressed tumor cells and 2) preventing nonspecific cell transduction to non-targeted normal cells. The cell transduction of TAT-Gel could, however, be efficiently reversed by addition of protamine. Feasibility of *in vivo* tumor targeting and "protamine-induced release" of TAT-Gel from the T84.66-Hep counterpart was confirmed by biodistribution and preliminary efficacy studies.

Conclusions—This study successfully demonstrated *in vitro* and *in vivo* the applicability of PTD-modified ATTEMPTS for toxin-based cancer therapy.

Keywords

Toxin; Protein transduction domains; Anti-CEA monoclonal antibody; Heparin; Cancer

INTRODUCTION

Since the first discovery of TAT peptide and its cell penetrating ability in 1988 (1), to date, numerous protein transduction domains (PTDs) have been synthesized or discovered (2-5). Due to the ability to deliver attached cargos (e.g. proteins, peptides and genes) into almost any type of cells (including brain and red blood cells) with an efficiency unmatched by other ligands (6-8), PTDs shed light to finally overcoming the cell membrane barrier, a major hindrance for many macromolecular drugs to exert their therapeutic efficacy (9-15). However, despite achieving certain successes in various research fields, clinical applications of PTDs has yet so far not been fully accomplished. One of the major impediments lies in the non-selectivity of the PTDs in their action of cell transduction (2, 16). When the excessive cell translocating ability of PTDs are projected to non-diseased normal cells, it can cause unwanted and, in some cases, severe toxicity if the attached cargoes do not have a selective mode of action in the diseased cells (16). Therefore to effectively curb the translocating activity of the PTDs and selectively deliver the PTD-conjugated drugs to the disease site has been an imminent task to be addressed. However, to date, despite the necessity and various efforts to develop an ideal delivery strategy to direct the PTD-modified cargos selectively to diseased cells, only a handful of approaches have yet shown success in truly achieving this goal (16-18).

PTD-modified ATTEMPTS (Antibody Targeted Triggered Electrically Modified Prodrug-Type Strategy), developed by Yang and co-workers, is a drug delivery strategy which strategically incorporates all the favorable features currently exploited by other drug delivery systems (DDS), 'active antibody targeting' and 'heparin/protamine-mediated prodrug', into a single system. Therefore, the DDS can provide maximum protection and selectivity, but still enables the utilization of the superior PTD-mediated cell transduction as the cell uptake mechanism (18-20). Therefore, the PTD-modified ATTEMPTS renders itself an ideal DDS for selective delivery of PTD-modified toxins to diseased cells. As depicted in Fig. 1, this drug delivery system (DDS) comprises of two compartments: a targeting antibody linked with a heparin molecule, and a drug part created by coupling a protein transduction domain (PTD) to the delivered drug (e.g. protein toxin). These two compartments automatically assemble into a tight complex *via* a charge/charge interaction

between the anionic heparin and cationic PTD. Binding with heparin would mask the cell-penetrating function of PTD due to inhibition of its adsorption to the cell surface. Hence, the complex would provide a prodrug behavior and avoid PTD-mediated uptake by normal tissues, alleviating drug-induced side effects. Following tumor targeting by the linked antibody, protamine sulfate, a clinical heparin antidote that binds heparin stronger than the PTD, will be administered to unmask heparin inhibition and restore the cell-internalization activity of the released PTD-toxin. Once within tumor cells, the toxin will induce apoptosis to only tumor cells.

Previously, we reported the development of a recombinant PTD-modified toxin chimera, TAT-gelonin (a.k.a. TAT-Gel) (21). Gelonin is a plant-derived toxin with exceptional N-glycosidase activity that can irreversibly inactivate eukaryotic ribosomes (22). Regarding the activity of gelonin, it was even reported, several gelonin molecules that can fully access the substrate ribosomes inside a tumor cell are sufficient to kill the cell (23). However, gelonin does not have any cell binding domain that can mediate the internalization into the tumor cells, and thus, by itself, is not effective for cancer treatment (21, 23). In a sharp contrast to gelonin, the TAT-Gel that we synthesized by attaching a renowned PTD, TAT peptide, to the gelonin by genetic recombination, could internalize various cancer cells while retained the N-glycosidase activity, and thus showed significantly enhanced anti-cancer activity (177-fold lower IC_{50} (avg. 54.3 nM)) (21). However, despite of excellent potency for killing tumor cells, due to the non-specificity in their cell uptake, a highly effective DDS was required for the safe administration of TAT-Gel.

To this regards, in this research, we explored the feasibility of applying the PTD-modified ATTEMPTS for effective yet safe administration of TAT-Gel, by utilizing a heparin functionalized anti-carcinoembryonic antigen (CEA) mAb, T84.66-Hep that showed feasible tumor targeting of TAT-Gel in our previous studies (24), as the targeting component and protamine as the trigger release agent. After *in vitro* characterization of the CEA binding specificity and cell internalization of T84.66-Hep, we prepared an antibody/toxin complex by mixing the T84.66-Hep and TAT-Gel. The functionality of the PTD-modified ATTEMPTS was assessed *in vitro via* confocal microscopy and cytotoxicity assays. Furthermore, the *in vivo* applicability of the PTD-modified ATTEMPTS for tumor targeting of TAT-Gel was examined using an LS174T xenograft tumor mouse model.

MATERIALS AND METHODS

Materials

Isopropyl-β-thiogalactopyranoside (IPTG) and carbenicillin were purchased from Fisher Scientific (Pittsburg, PA). Traut's reagent (2-iminothiolane), heparin sulfate, MES (2-(*N*-morpholino) ethanesulfonic acid), EDC (1-Ethyl-3-[3-dimethylaminopropyl]carbodiimide Hydrochloride) and TRITC (rhodamine B isothiocyanate) were purchased from Sigma-Aldrich (St. Louis, MO). BL21star (DE3) *E. coli* strain, AcTEV™ protease, Hybridoma serum free medium (SFM), Dulbecco's Modified Eagle Medium (DMEM), fetal bovine serum albumin (FBS) and PBS (pH 7.4) were purchased from Invitrogen (Carlsbad, CA). Dylight 488 and Dylight 775-B4 were purchased from Thermo Scientific (Rockford, IL).

PEG (NH_2-PEG-MAL; 3.5 kDa) was purchased from JenKem Technology USA Inc. (Allen, TX).

Expression and purification of recombinant TAT-gelonin chimera (TAT-Gel)

Expression and purification of TAT-Gel from *E. coli* was by following the identical procedures described in Shin *et al* (21). Briefly, a single colony of BL21 (DE3) *E. coli* transformed with pET-TAT-Gel vector was picked and used to inoculate 20 mL LB medium containing 50 μg/mL carbenicillin. After overnight incubation at 37°C, this starter culture was diluted to 1 L with fresh LB medium, and the large (1L) culture was incubated under the same conditions. When the optical density at 600 nm (OD_{600}) reached 0.7 – 1, IPTG (at a final concentration of 0.5 mM) was added for induction of the expression of TAT-Gel. The culture was further maintained for 6 h, and then the *E. coli* cells were harvested by centrifugation (4000 rpm for 20 min). After re-dispersion in 20 mM PBS (300 mM NaCl, pH 7), cells were lysed by sonication and the lysates were centrifuged, and the supernatant containing the soluble thioredoxin-6×His tagged TAT-gelonin (a.k.a. TRX-TAT-Gel) was collected and loaded onto Ni-NTA resins (HisPure® Ni-NTA resin, Bio-Rad Laboratories, Hercules, CA). After washing the resins with 20 mM PBS, TRX-TAT-Gel was eluted with imidazole (20 mM PBS, 300 mM NaCl, 400 mM imidazole, pH 7). The final TAT-Gel product was acquired after cleavage of the thioredoxin-6xHis tag *via* incubation of the TRX-TAT-Gel with TEV protease (AcTEV™ protease, Invitrogen) and subsequent heparin column (HiTrap Heparin HP, GE Healthcare Bio-Sciences, Pittsburgh, PA) purification with salt gradient elution. TAT-Gel was kept in 4°C refrigerator until further use. Recombinant gelonin was expressed and purified following the procedures described in Shin *et al* (21).

Production of T84.66

T84.66, a murine anti-CEA monoclonal antibody, was produced from hybridoma cells (ATCC # HB-8747, Manassas, VA) following the procedures described in Urva *et al* (25). Briefly, hybridoma cells were grown in SFM in a 2L spinner flask and, at every third day, the supernatant containing the T84.66 was collected and loaded onto a protein G affinity column (Protein G Sepharose™ 4 Fast Flow, GE Healthcare Biosciences, Pittsburg, PA) pre-equilibrated with 20 mM phosphate buffer (PB). After wash with 200 mL of PB, T84.66 was eluted with 0.1 M glycine buffer (pH 2.8) in a tube containing 1 M Tris buffer (pH 9) for immediate neutralization of the elution buffer and dialyzed against PBS (20 mM, 0.15 M NaCl, pH 7.4).

Synthesis of T84.66-heparin chemical conjugate (T84.66-Hep)

Heparin was chemically conjugated to T84.66 *via* a thioether bond using hetero-bifunctional polyethylene glycol (PEG) as the cross-linker. For heparin activation, heparin (40 mg/mL in 0.1 M MES buffer, pH 5) was mixed with 5-fold molar excess of PEG (NH_2-PEG-MAL, 3.4 kDa) and 100-fold molar excess of EDC, and then the reaction mixture was incubated for 2 h at room temperature. The heparin-PEG-MAL was purified by using anion exchange chromatography (Bio-Scale™ Mini UNOsphere™ Q Cartridge, Bio-Rad Laboratories, Hercules, CA). At the same time, T84.66 was thiol-activated by incubating T84.66 (10 mg/mL, 50 mM HEPES buffer, 5 mM EDTA, pH 8) with 10-fold molar excess of Traut's

reagent for 1 h at room temperature. Any unreacted Traut's reagent was removed by ultrafiltration (molecular weight cut off (MWCO): 10 kDa), and the generated thiol groups were quantified by Ellman's assay. The prepared thiol-activated T84.66 (T84.66-SH) was mixed with 5-fold molar excess of heparin-PEG-MAL, and the conjugation reaction mixture was incubated for overnight at room temperature. After incubation, the T84.66-Hep was purified from T84.66-SH by anion exchange chromatography using a salt gradient (0 to 2 M NaCl at a rate of 0.02M/min, flow rate: 1 mL/min). In addition, any unreacted heparin and heparin-PEG-MAL were removed by ultrafiltration (MWCO: 100 kDa). The purification steps for synthesis of T84.66-Hep were monitored by SDS-PAGE analysis, and the T84.66 and heparin amounts consisting of the final T84.66-Hep product were quantified by measuring the optical density at 280 nm (OD_{280}) and azure A assay (26), respectively.

Cell culture

LS174T (high expression of CEA) and HCT116 (low expression of CEA) human adenocarcinoma cell lines were purchased from American Type Culture Collection (ATCC) (Manassas, VA). The cell cultures were maintained in DMEM containing 1% (v/v) penicillin-streptomycin and 10% FBS.

Fluorescence dye labeling

For labeling of T84.66-Hep, TAT-Gel and gelonin with fluorescence dyes (e.g., rhodamine B isothiocyanate (TRITC), Dylight 488 or Dylight 775-B4), protein samples (5 mg/mL in 20 mM sodium biocarbonate buffer; pH 9.3) were mixed with 5-fold molar excess of dyes and incubated for 2 h at room temperature. After incubation, unreacted excessive dyes were removed by using dye removal resins (Thermo Scientific, Rockford, IL).

Cellular analyses of T84.66-Hep binding selectivity and internalization

LS174T and HCT116 cells were seeded on 24-well plates at a density of 2×10^4 cells per well and incubated for overnight. To visually observe the cellular association of the T84.66-Hep, when cells were attached on the bottom of the plates, TRITC labeled-T84.66-Hep (at 5 μM concentration) were added to the wells and incubated at 37°C for 2 h. After wash with PBS, the nuclei of the cells were counterstained with Hoechst 33342. The images of the live cells were acquired by using a fluorescence microscope (Nikon Eclipse TE2000S inverted fluorescence microscope) and analyzed with Metamorph software (Molecular Devices Corporation, Sunnyvale, CA). In addition, to quantitatively evaluate the total cell associated and internalized fraction of T84.66-Hep amount along the time course, LS174T and HCT116 cells were incubated with TRITC-labeled T84.66-Hep and incubated at 37°C up to 48 h. At intended time points (0, 0.5, 1, 2, 6, 12, 24 and 48 h), cells were detached from the wells and transferred to eppendorf tubes. To measure the total cell associated amount of T84.66-Hep, the cells were lysed after PBS wash, and the fluorescence intensity was measured using a plate reader (BioTek® Synergy™ BioTek, Co., Winooski, VT). For quantification of cell internalized T84.66-Hep, cells prepared in the tubes were incubated with glycosylphosphatidylinositol (GPI)-specific phospholipase C (Sigma Aldrich, St. Louis, MO), washed with 0.5 M NaCl/0.1 M acetic acid (27) and then, after lysis, the fluorescence intensity was measured.

In vitro assessment of the PTD-modified ATTEMPTS

LS174T and HCT116 cells were seeded on Nunc™ Lab-Tek™ Chambered Coverglass (Thermo Scientific) at a density of 10^4 cells per well and incubated for overnight. After incubation, cells were treated with either TRITC-labeled gelonin, TRITC labeled-TAT-Gel or TRITC labeled-TAT-Gel/Dylight 488 labeled-T84.66-Hep complex (a.k.a. TAT-Gel/T84.66-Hep) and then incubated at 37°C for 3 h. Final concentrations of gelonin and TAT-Gel were 1 μM, and the TAT-Gel/T84.66-Hep was prepared by mixing the two components at 1:3 molar ratios (TAT : heparin). For a group of LS174T cells pre-treated with TAT-Gel/T84.66-Hep, protamine (3-fold molar excess of heparin) was added to the wells immediately following the complex treatment. After incubation, cells were washed with PBS and the nuclei of the cells were counterstained with Hoechst 33342. The images of live cells were acquired by using a Nikon A1R-A1 confocal laser microscope (Nikon Instruments Inc., Melville, NY) with a 60× objective and analyzed using NIS-Elements microscope imaging software (Nikon Instruments Inc., Melville, NY).

T84.66-Hep/protamine-mediated modulation of TAT-Gel-induced cytotoxicity

LS174T cells were dispensed into 96-well plates at a density of 5×10^3 cells per well and incubated for overnight. The next day, cells were treated with either: 1) TAT-Gel, 2) protamine (a.k.a. Pro), 3) TAT-Gel with protamine (a.k.a. “TAT-Gel+Pro”), 4) T84.66-Hep, 5) TAT-Gel/T84.66-Hep complex or 6) TAT-Gel/T84.66-Hep with protamine (“TAT-Gel/T84.66-Hep+Pro”). TAT-Gel/T84.66-Hep complex was prepared by mixing TAT-Gel with increasing molar ratios of T84.66-Hep (TAT : heparin = 5:1, 3:1, 1:1 and 1:3) and incubation for 30 min at 4°C. For evaluation of the protamine effect on reversal of the T84.66-Hep inhibition for the cell transduction of TAT-Gel, protamine was added to the cells pre-treated with TAT-Gel/T84.66-Hep (TAT : heparin molar ratio = 3:1) with different heparin-to-protamine molar ratios (10:1, 5:1, 1:1 and 1:2). For “TAT-Gel+Pro” treatment, protamine was added to the TAT-Gel pre-treated cells with 1:1 molar ratio. After treatment with the test compounds, cells were incubated at 37 °C for 48 h, and the relative cell proliferation was measured by XTT assay. In addition, to evaluate the time dependency of protamine addition time on the effects of protamine triggered release, LS174T cells were incubated with TAT-Gel/T84.66-Hep complex (TAT-Gel concentration: 100 nM; molar ratio of TAT to heparin = 3:1) for 6 h, and then, after wash with PBS, protamine (2-fold molar excess to heparin) was added to the wells at different time points (0, 2, 6, 24 and 48 h). The cells were incubated at 37 °C for total 72 h since addition of the complex to the wells, and the relative cell proliferation was measured by XTT assay.

LS174T s.c. xenograft tumor mouse model

Male athymic nude mice (body weight: 23 - 27 g) were purchased from Charles Rivers Laboratories (Raleigh, NC). Mice were housed in sterile animal facilities and fed by standard chow diet. At day 0 (three days after arrival), LS174T cells (5×10^6 cells/mouse) were implanted (*s.c.*) in the left flank regions of the mice. Specifically for biodistribution studies, after tumor implantation, mice were fed by special alfalfa-free diet (AIN-76A rodent diet, gamma-irradiated, Research Diets, Inc, New Brunswick, NJ) to reduce the autofluorescence during the tissue imaging (28). Tumor size was measured using a vernier

caliper, and the volume was calculated by the formula of V (mm^3) = ($w^2 \times l$) / 2. In the equation, V is the tumor volume, w is the width and l is the length of the tumor.

Biodistribution studies

The tissue distribution profiles of TAT-Gel, when administered alone and complexed with T84.66-Hep, were examined with LS174T xenograft tumor bearing mice. When the average tumor size reached 500 mm^3, mice (N = 5) were administered with either 5 mg/kg of TAT-Gel-B4 or 2) TAT-Gel-B4/T84.66-Hep (5 mg/kg of TAT-Gel-B4/11 mg/kg of T84.66-Hep) *via* tail vein injection. The mice injected with TAT-Gel-B4 were euthanized at 15 min, 1, 5 and 24 h post-injection, and the TAT-Gel-B4/T84.66-Hep injected mice were euthanized at 2, 24, 48 and 72 h post-injection, and then the major organs (e.g., tumor, heart, liver, spleen, lung, kidney and intestine) were harvested. The fluorescence intensities of the organs were measured immediately by using the IVIS® spectrum imaging system (Xenogen, Alameda, CA). Ex/Em wavelength of 745 nm/800 nm, binning (8), exposure time (2 s), *f*/stop (1) and fields of view (25 cm × 25 cm) were used identically for imaging all the organs. The fluorescence images were analyzed using Living Image 2.5 software (Xenogen, Alameda, CA) and mean fluorescence intensities (M.F.I.s) of the organs were calculated by subtracting the mean fluorescence intensity of the corresponding tissue from a blank mouse. The M.F.I.s were normalized by the tissue weights.

In vivo evaluation of PTD-modified ATTEMPTS

Three days after tumor implantation (at day 3) when average tumor size reached 40 mm^3, LS174T xenograft tumor mice were randomly divided into 5 groups (N = 10) and treated with: 1) PBS, 2) TAT-Gel (7 mg/kg), 3) TAT-Gel/T84.66-Hep (7 mg/kg TAT-Gel/21 mg/kg T84.66-Hep), 4) “TAT-Gel/T84.66-Hep+Pro” (7 mg/kg TAT-Gel/21 mg/kg T84.66-Hep and 10 mg/kg protamine) or 5) protamine (a.k.a. “Pro”, 10 mg/kg). Mice were treated three times with the above recipe at day 3, 6 and 9 *via* tail vein injection. For the “TAT-Gel/T84.66-Hep+Pro” treatment, protamine was injected to TAT-Gel/T84.66-Hep administered mice *via* tail vein at 24 h post-injection of the complex. Tumor sizes and body weights of the mice were measured daily. All animal experiments were conducted according to protocols approved by the University of Michigan Committee on Use and Care of Animals (UCUCA).

Statistical analysis

All data are expressed as mean ± standard deviation. An unpaired Student's t-test was used for comparison of the cell associated amounts of T84.66-Hep, and 1-way ANOVA (Tukey's multiple comparison test as the post hoc test) was used in the cytotoxicity and efficacy studies. $P < 0.05$ was considered significant.

RESULTS

Expression and purification of TAT-gelonin chimera (TAT-Gel)

TAT-Gel was successfully produced from *E. coli* as a soluble and functional protein and purified by using Ni-NTA metal affinity chromatography. The purified thioredoxin-6×His tagged TAT-gelonin (TRX-TAT-Gel) was incubated with AcTEV™ protease (Invitrogen) for removal of the thioredoxin-6×His tag, and the final TAT-Gel product was acquired after

subsequent purification with heparin column as a single peak fraction (at 0.7 M NaCl) using salt gradient elution (0 to 2 M NaCl) (data not shown).

Synthesis of T84.66-heparin chemical conjugate (T84.66-Hep)

T84.66 and heparin were chemically conjugated *via* a stable thio-ether bond formed between thiol-activated T84.66 (T84.66-SH) and heparin derivatized with maleimide groups (Hep-PEG-MAL). The T84.66-Hep conjugate was successfully purified from unreacted T84.66-SH by using anion exchange chromatography (Q Cartridge, Bio-Rad Laboratories, Hercules, CA) with salt gradient elution (0 to 2 M NaCl). While the unreacted T84.66 was eluted initially with no salt, T84.66-Hep was eluted with 0.8 - 1.8 M NaCl (data not shown). After removal of heparin and heparin-PEG-MAL contained in the T84.66-Hep peak fraction by ultrafiltration, the final T84.66-Hep product was acquired. The production yield for T84.66-Hep was 38% (3.8 mg conjugate based on 10 mg T84.66 used), and the average conjugation molar ratio of T84.66 to heparin was 1:3.

Cell binding selectivity and internalization of T84.66-Hep

To evaluate the selective binding of T84.66-Hep to CEA overexpressing tumor cells, TRITC-labeled T84.66-Hep was incubated with CEA low expression (HCT116) and high expression (LS174T) cells, and the fluorescence images of the cells were acquired by fluorescence microscopy. In addition, the total cell associated and internalized amounts of T84.66-Hep along the time course were quantified by measuring the fluorescence intensities of the cell lysates after different washing procedures. As shown in Fig. 2A, while little, if any fluorescence signal was observed from the HCT116 cells, apparent binding of T84.66-Hep to LS174T cells was observed. After 6 h of incubation, the cell associated amounts of T84.66-Hep reached a plateau, and a significant difference (5.8-fold) in the fluorescence intensities was observed between LS174T and HCT 116 cells (Fig. 2B). Despite significant binding to the cell surface of LS174T cells, however, cell internalization was limited to 35% of the cell-associated T84.66-Hep after 48 h of incubation; which suggested that the majority of the T84.66-Hep remained on the LS174T tumor cell surface but did not enter the cells.

In vitro evaluation of PTD-modified ATTEMPTS

After preparation and characterization of the drug (TAT-Gel) and targeting (T84.66-Hep) components, the feasibility of ‘targeting’ and ‘prodrug’ features of the drug delivery system (DDS) were assessed using confocal microscopy. As shown in Fig. 3, whereas no fluorescence signal was observed from HCT116 and LS174T cells after incubation with gelonin (A & D), significant internalization of TAT-Gel (B & E) was observed from both the cell lines, indicating effective yet nonselective mode of cell transduction of TAT-Gel. However, when HCT116 cells were incubated with TAT-Gel/T84.66-Hep (C), little fluorescence intensity was observed, suggesting that the T84.66-Hep completely blocked the cell transduction of TAT-Gel, and thus TAT-Gel remained as an “inactive prodrug” outside the cells. In comparison to the HCT116 cells, LS174T cells incubated with TAT-Gel/T84.66-Hep exhibited apparent binding of both components to the cell membrane; as observed from the superimposed fluorescence signals (F & G) on the boundary of the cells.

These results indicated that TAT-Gel/T84.66-Hep could bind selectively to CEA overexpressed tumor cells as a stable complex yet remained on the cell surface rather than internalized. In a sharp contrast, when protamine was added to the LS174T cells treated with the TAT-Gel/T84.66-Hep, while T84.66-Hep (H) was remaining on the cell membrane, significant internalization of TAT-Gel (I) was observed; suggesting that protamine was able to release TAT-Gel from the T84.66-Hep counterpart, and the freed TAT-Gel internalized cells as an "active drug".

T84.66-Hep and protamine effects on cytotoxicity induced by TAT-Gel

The modulating effects of 'T84.66-Hep binding' and 'protamine-induced release' on TAT-Gel-induced cytotoxicity were evaluated on LS174T cells. The results are shown in Fig. 4 and the IC_{50} values are summarized in Table 1. Treatment of cells with TAT-Gel/T84.66-Hep showed no cell death (up to 5 μM of TAT-Gel) at above 3:1 molar ratio (TAT : heparin), while significant cytotoxicity (IC_{50} = 29.2 ± 7.9 nM) was observed by treatment of TAT-Gel alone (Fig. 4A). In comparison, when protamine (a.k.a. "Pro") was added to the cells pre-treated with the TAT-Gel/T84.66-Hep, significantly enhanced cytotoxic effect was observed. Notably, at above heparin-to-protamine molar ratio of 5:1, the IC_{50} values by the "TAT-Gel/T84.66-Hep+Pro" treatment were similar to that of the TAT-Gel (Fig. 4B). To assess the time dependency of protamine addition time on the effects of the protamine-induced release, when the LS174T cells pre-treated with TAT-Gel/T84.66-Hep were incubated with protamine given at different time points (0, 2, 6, 24, 48 h), significant cell death was observed throughout all the protamine-treated cells, compared with the cells not treated with protamine (Fig. 4C). However, no statistical difference was observed regarding the cell viability among the protamine-treated groups.

Biodistribution studies

Biodistribution profiles of TAT-Gel, when administered alone and complexed with T84.66-Hep, were examined with LS174T xenograft tumor bearing nude mice. Fig. 5A and 5C show the representative images of dissected major organs harvested from the mice administered with Dylight 775-B4-labeled TAT-Gel (a.k.a. TAT-Gel-B4) at 15 min, 1, 5 and 24 h post-injection and the weight normalized mean fluorescence intensities (M.F.I.s) of the organs, respectively. Fig. 5B and 5D exhibit the representative organ images from the mice administered with TAT-Gel-B4/T84.66-Hep at 2, 24, 48 and 72 h post-injection and the weight normalized M.F.I.s of the organs, respectively. When TAT-Gel-B4 was administered alone, rapid tissue distribution and elimination was observed from the body. As can be seen from Fig. 5A and 5C, even at 15 min post-injection, only minimal fluorescence intensity was observed from the heart which reflects the fluorescence intensity from the blood (29). TAT-Gel-B4 was mainly distributed to kidney and liver, and only a weak fluorescence signal was observed from the tumor up to 5 h (Fig. 5A & 5C). In a sharp contrast, when TAT-Gel-B4/T84.66-Hep was administered, TAT-Gel-B4 showed significantly prolonged residence in the blood circulation; as implicated by the presence of a traceable amount of fluorescence signal from the heart even at 24 h post-administration. At 2 and 24 h post-injection of TAT-Gel-B4/T84.66-Hep, TAT-Gel-B4 was observed in most of the organs (e.g., kidney, tumor, spleen, liver, heart and intestine), but, at 48 h post-administration, only visible from tumor, liver and kidney (Fig.5B & 5D). By 48 h post-administration of TAT-Gel-B4/T84.66-Hep,

the tumor-to-heart ratio of the weight normalized M.F.I. increased up to 17-fold (from 1.0 at 2 h post-administration to 17.1); suggesting that active targeting of TAT-Gel was indeed achieved by complexation with T84.66-Hep. In result, remarkably, a 43-fold higher tumor exposure (AUC_{tumor}) was observed by administration of the TAT-Gel-B4/T84.66-Hep, compared with injection of TAT-Gel-B4 alone.

In vivo evaluation of PTD-modified ATTEMPTS with LS174T xenograft bearing mice

To evaluate the feasibility of applying PTD-modified ATTEMPTS for effective yet safe delivery of TAT-Gel to tumor, a preliminary efficacy study was conducted using LS174T xenograft tumor mouse model. As shown in Fig. 6A and 6B, at day 40, mice administered with TAT-Gel (1770 ± 470 mm^3; 13% reduction) and protamine (1920 ± 437 mm^3; 6% reduction) showed no statistically significant differences in their tumor volumes compared with those of the control PBS-treated mice (2042 ± 410 mm^3), indicating there were little therapeutic effects by neither TAT-Gel nor protamine alone. In comparison, the mice treated with TAT-Gel/T84.66-Hep (1270 ± 419 mm^3 at day 40; $p < 0.01$**; 38% reduction) showed a significant inhibition in tumor growth; presumably contributed by enhanced tumor accumulation and release of a portion of TAT-Gel from the T84.66-Hep counterpart on the tumor cell surface. However, it was the mice treated with a combination of TAT-Gel/T84.66-Hep and protamine (a.k.a. “TAT-Gel/T84.66-Hep+Pro”; protamine administration at 24 h-post injection of TAT-Gel/T84.66-Hep) which exhibited the greatest therapeutic effects (707 ± 289 mm^3 at day 40, $p < 0.001$***; 65% reduction). Statistically significant difference was observed in the tumor volumes between the two groups of TAT-Gel/T84.66-Hep and “TAT-Gel/T84.66-Hep+Pro” ($p < 0.05$*).

During the efficacy studies, the average body weight of the mice in all the groups increased from 25.1 ± 2.2 g at day 0 to 33.3 ± 1.8 g at day 40. As shown in Fig. 6C, the average body weight of protamine-treated mice was similar to that of control (PBS-treated) mice along the time course. However, mice treated with TAT-Gel, T84.66-Hep/TAT-Gel and “T84.66-Hep/TAT-Gel+Pro” experienced loss of body weight by the treatment. Specifically, when compared the average body weights at day 10 (the next day after the last treatment), TAT-Gel-treated mice (20% weight loss; $p < 0.001$***) showed the most severe loss during the treatment, followed by mice treated with “TAT-Gel/T84.66-Hep+Pro” (15% weight loss; $p < 0.001$***) and TAT-Gel/T84.66-Hep (7% weight loss; $p < 0.05$*).

DISCUSSION

Due to the unmatched transduction efficiency, protein transduction domains (PTDs; e.g. LMWP and TAT) offered an exceptional method for intracellular delivery of various macromolecular drugs (e.g., proteins, peptides and genes, etc.) (9, 30-35). However, the lack of selectivity in their cell internalization can severely halt the clinical application of those PTD-modified drugs, especially when the drugs (e.g. protein toxins) do not have selectivity in their mode of action only to the diseased cells, because of the concerns of introducing severe drug-associated toxicity on normal tissues (9, 16). To this regards, in this research, we explored the feasibility of applying PTD-modified ATTEMPTS (Antibody Targeted Triggered Electrically Modified Prodrug-Type Strategy) (18), a drug delivery strategy based

on 1) active antibody targeting, 2) heparin/protamine-mediated prodrug and 3) PTD-mediated cell transduction, for effective yet safe administration of a PTD-modified toxin chimera, TAT-gelonin (a.k.a. TAT-Gel) for cancer therapy (Fig. 1).

Two crucial factors which must be maximally optimized to practically realize a clinically effective anti-cancer drug therapy by the PTD-modified ATTEMPTS are: efficiency of antibody targeting and extent of prodrug protection. The first issue relates to antibody targeting, in order to reach a clinically needed therapeutic efficacy but limited drug-induced toxicity, tumor targeting of the antibody must be sufficiently high. This problem could be answered by adopting a highly effective mAb (e.g. T84.66) for the targeting moiety. Carcinoembryonic antigen (CEA) has been shown to be involved in tumor growth and metastasis, mediation of cell-cell adhesion, and recognition of tumors and apoptotic pathway by the immune system (36). It is a glycosylated cell surface antigen known to be significantly over-expressed in certain adenocarcinomas including colorectal cancer, while displaying limited expression in normal tissues from which the tumor originates (36, 37). This differential expression offers a means for discriminating tumor cells from normal tissues, rendering CEA an extremely attractive target for antibody-directed tumor therapy. Indeed, T84.66, a mouse monoclonal antibody developed against human CEA, displayed a very high affinity ($K_a = 2.6\times10^{10}\ M^{-1}$) and targeting specificity toward CEA-expressing tumors (38). In a previous study comparing the plasma pharmacokinetics of T84.66 in control and CEA-expressing LS174T xenograft bearing mice, at low doses (e.g. 1 mg/kg), it was reported that greater than 85% of the injected T84.66 dose accumulated at the tumor target, exemplifying an extraordinarily targeting efficiency toward colorectal tumors (39). Aside from this unmatched targeting specificity, another crucial merit of T84.66 was being a non-internalizing mAb, as its actions to inhibit tumor growth stem from blocking the establishment of new metastatic sites and cell proliferation (27). This non-internalizing property endows us to exploit the maximum extent of protamine-induced release of TAT-Gel targeted to the tumor cells. Importantly, through cellular studies (Fig. 2A and 2B), we found that, after heparin conjugation, T84.66 still retained those important properties of specific CEA binding and non-internalization. After incubation with TRITC-labeled T84.66-Hep, significantly higher fluorescence intensity was observed from CEA high expression (LS174T) cells than low expression (HCT116) cells, which clearly evidenced the targeting ability of T84.66-Hep to CEA overexpressed cancer cells. Moreover, quantitative analyses of the cell associated and internalized amounts of T84.66-Hep (Fig. 2B), showed that, up to 48 h, the majority (65% at 48 h) of T84.66-Hep remained on the cell surface and were available for protamine activation.

The ‘prodrug’ feature of the DDS is modulated by two components, heparin and protamine. Heparin, a biocompatible polymer with exceptionally high density of negative charge residues on the molecule surface, strongly yet reversibly binds with highly cationic PTDs and neutralizes their positive charge essential for cell transduction (18). Thus, the heparin/PTD interaction provides an effective means for safe delivery of PTD-modified toxins to the tumor site as an ‘inactive prodrug’ unable to exert any toxicity to non-targeted normal cells. Once targeted, however, this heparin/PTD binding needs to be efficiently reversed for the PTD-modified toxins to enter tumor cells. For the triggered release of the PTD-toxins, protamine, a clinical antidote used for heparin intoxication, is an ideal agent

because protamine has much stronger affinity to heparin than cationic PTDs (e.g. TAT and LMWP) (20, 25). In this study, the prodrug feature of the DDS was evaluated by confocal microscopy (Fig. 3) and cytotoxicity studies (Fig. 4). The confocal images of the cells apparently showed that TAT-Gel can internalize cells, regardless of whether they are CEA low expression (HCT116) (Fig. 3B) or high expression (LS174T) (Fig. 3E). However, neither of the cells incubated with TAT-Gel/T84.66-Hep, exhibited internalization of TAT-Gel. While HCT116 cells showed neither binding nor internalization of TAT-Gel (Fig. 3C); as the TAT-Gel/T84.66-Hep cannot bind to the cells, in case of LS174T cells, the complex was able to bind but remained on the cell surface (Fig. 3F and 3G). The consequence of the heparin blocking of the internalization of TAT-Gel was clearly realized from the cytotoxicity studies. Complexes prepared by increasing TAT-to-heparin molar ratios (from 5:1 to 1:3) exhibited significantly attenuated cytotoxicity (Fig. 4A). Specifically, at above TAT-to-heparin molar ratios of 3:1, the TAT-Gel/T84.66-Hep yielded no cytotoxicity (up to 5 μM of TAT-Gel), suggesting that TAT-Gel cell internalization was completely blocked by the T84.66-Hep. In a sharp contrast, when protamine, the trigger agent, was added to the LS174T cells pre-treated with TAT-Gel/T84.66-Hep, significant uptake of TAT-Gel was observed (Fig. 3H and 3I) and led to remarkably enhanced anti-cancer effects (Fig. 4B). Importantly, this protamine-induced release of TAT-Gel from the T84.66-Hep counterpart on the LS174T cell surface was available even 48 h after the complex was bound to the cells (Fig. 4C), suggesting the presence of a timely window for the protamine administration after the TAT-Gel/T84.66-Hep complex is cleared from the blood circulation.

Encouraged by the *in vitro* feature characterizations of the PTD-modified ATTEMPTS,the feasibility of the approach was further evaluated *in vivo* by examining the biodistribution, efficacy and toxicity using LS174T xenograft tumor bearing mice. The biodistribution study results (Fig. 5) provided us with a convincing evidence of tumor targeting by means of the DDS. Remarkably, a 43-fold enhancement in tumor exposure (AUC_{tumor}) of TAT-Gel was accomplished by administration of the complex. This significant increase in the tumor accumulation appears not only due to the successful active targeting mediated by T84.66, but also stems from the dramatic change in the plasma residence time of the TAT-Gel by forming a complex with T84.66-Hep. Indeed, by administration as TAT-Gel/T84.66-Hep complex, TAT-Gel exhibited a significantly prolonged residence in the blood as well as other major organs; as evidenced by the fluorescence intensity observed from the heart up to 24 h, compared with minimal detection from the heart dissected from the mice administered with TAT-Gel alone even at 15 min. This dramatic increase of TAT-Gel residence in the blood circulation can be highly beneficial for the treatment as it can provide a much greater opportunity for passive targeting that relies on the enhanced permeation and retention (EPR) effect, especially for drugs, such as toxins with extremely short plasma half-lives (< 5 min) (40). Based on all the evidences gathered from our experiences, the proof-of-concept of the feasibility of the DDS for application to toxin-based cancer therapy was assessed *via* a preliminary *in vivo* efficacy study with LS174T xenograft bearing mice (Fig. 6). While TAT-Gel yielded no therapeutic effect, presumably due to insufficient tumor accumulation (Fig. 5A and 5C), the mice treated with TAT-Gel/T84.66-Hep and “TAT-Gel/T84.66-Hep +Pro” exhibited significant inhibition of tumor growth (38% inhibition of tumor growth, $p < 0.01$**, 65% inhibition of tumor growth, $p < 0.001$***, respectively). While these results

demonstrated the significance of targeting for enhanced therapeutic effects, the highest therapeutic effect by the “TAT-Gel/T84.66-Hep+Pro” treatment substantiated our hypothesis that protamine can reverse the inhibition of T84.66-Hep block and free the TAT-Gel to enter the tumor cells.

Despite the beneficial therapeutic effects by protamine administration, the study results also revealed potential toxicity concerns if any “prodrug” can be activated by protamine in the blood circulation or normal tissues; evidenced by a significantly higher toxicity observed from the mice treated with “TAT-Gel/T84.66-Hep+Pro”compared with TAT-Gel/T84.66-Hep-treated mice (Fig 6C). To this regards, extensive animal studies accompanied with physiologically-based pharmacokinetic (PBPK) modeling are currently ongoing by our research group for optimizing the time for protamine administration.

CONCLUSION

In this research, we demonstrated the feasibility to apply PTD-modified ATTEMPTS for toxin therapy for the treatment of cancer, by using a heparin-functionalized non-internalizing anti-CEA mAb, T84.66-Hep, and a recombinant PTD-modified toxin chimera, TAT-Gel. Confocal microscopy and cytotoxicity assay results confirmed that the essential features of the PTD-modified ATTEMPTS, ‘antibody targeting’ and ‘heparin/protamine-mediated prodrug’ were applicable for selectively delivering a recombinant PTD-modified toxin chimera, TAT-Gel, to CEA high expression cells (LS174T). Biodistribution and preliminary efficacy studies further showed that by, administration of TAT-Gel as a complex with T84.66-Hep, when compared with administration of TAT-Gel alone, significantly higher (43-fold) tumor accumulation was available, while exhibiting significantly lower toxicity. Furthermore, by administration of protamine to the TAT-Gel/T84.66-Hep pre-treated mice (at 24 h post-administration), a significant (65%) inhibition of tumor growth was accomplished. Overall, this research demonstrated an effective yet safer way to deliver highly potent toxins to tumor *via* utilizing the PTD-modified ATTEMPTS.

Supplementary Material

Refer to Web version on PubMed Central for supplementary material.

ACKNOWLEDGEMENTS

The authors thank Dr. Wolfgang E. Trommer (University of Kaiserslautern, Germany) for gelonin expression vector (pET28a-Gel). This work was partially supported by the NSFC 2013 A3 Foresight Program (81361140344) and National Key Basic Research Program of China (2013CB932502). In addition, this work was also supported in part by National Institutes of Health R01 Grants CA114612.

ABBREVIATIONS

ATTEMPTS	Antibody Targeted Triggered Electrically Modified Prodrug-Type Strategy
CEA	Carcinoembryonic antigen
DDS	Drug delivery system

DMEM	Dulbecco's Modified Eagle Medium
EDC	1-Ethyl-3-[3-dimethylaminopropyl] carbodiimide
EDTA	Ethylenediaminetetraacetic acid
FBS	Fetal bovine serum albumin
HEPES	4-(2-hydroxyethyl)-1-piperazineethanesulfonic acid
IPTG	Isopropyl-β-thiogalactopyranoside
mAb	Monoclonal antibody
MES	2-(*N*-morpholino) ethanesulfonic acid
M.F.I.	Mean fluorescence intensity
PEG	Polyethylene glycol
Pro	Protamine
PTD	Protein transduction domain
SFM	Hybridoma serum free medium
T84.66-Hep	T84.66-heparin chemical conjugate
TAT-Gel	Recombinant TAT-gelonin fusion chimera
TRX-TAT-Gel	Recombinant thioredoxin-6×His tagged TAT-gelonin fusion chimera

REFERENCES

1. Frankel AD, Pabo CO. Cellular uptake of the tat protein from human immunodeficiency virus. Cell. 1988; 55:1189–93. [PubMed: 2849510]
2. Shin MC, Zhang J, Min KA, Lee K, Byun Y, David AE, et al. Cell-penetrating peptides: achievements and challenges in application for cancer treatment. J Biomed Mater Res. 2014; 102:575–87.
3. Lindgren M, Hallbrink M, Prochiantz A, Langel U. Cell-penetrating peptides. Trends Pharmacol Sci. 2000; 21:99–103. [PubMed: 10689363]
4. Milletti F. Cell-penetrating peptides: classes, origin, and current landscape. Drug Discov Today. 2012; 17:850–60. [PubMed: 22465171]
5. Patel LN, Zaro JL, Shen WC. Cell penetrating peptides: intracellular pathways and pharmaceutical perspectives. Pharm Res. 2007; 24:1977–92. [PubMed: 17443399]
6. Schwarze SR, Ho A, Vocero-Akbani A, Dowdy SF. In vivo protein transduction: delivery of a biologically active protein into the mouse. Science. 1999; 285:1569–72. [PubMed: 10477521]
7. Kwon YM, Chung HS, Moon C, Yockman J, Park YJ, Gitlin SD, et al. L-Asparaginase encapsulated intact erythrocytes for treatment of acute lymphoblastic leukemia (ALL). J Control Release. 2009; 139:182–9. [PubMed: 19577600]
8. He H, Ye J, Wang Y, Liu Q, Chung HS, Kwon YM, et al. Cell-penetrating peptides meditated encapsulation of protein therapeutics into intact red blood cells and its application. J Control Release. 2014; 176:123–32. [PubMed: 24374002]
9. Shin MC, Zhang J, David AE, Trommer WE, Kwon YM, Min KA, et al. Chemically and biologically synthesized CPP-modified gelonin for enhanced anti-tumor activity. J Control Release. 2013; 172:169–78. [PubMed: 23973813]
10. Meade BR, Dowdy SF. Exogenous siRNA delivery using peptide transduction domains/cell penetrating peptides. Adv Drug Deliv Rev. 2007; 59:134–40. [PubMed: 17451840]

11. Lehto T, Kurrikoff K, Langel U. Cell-penetrating peptides for the delivery of nucleic acids. Expert Opin Drug Del. 2012; 9:823–36.
12. Madani F, Lindberg S, Langel U, Futaki S, Graslund A. Mechanisms of cellular uptake of cell-penetrating peptides. J Biophys. 2011:414729. [PubMed: 21687343]
13. Snyder EL, Dowdy SF. Cell penetrating peptides in drug delivery. Pharm Res. 2004; 21:389–93. [PubMed: 15070086]
14. Yuan X, Lin X, Manorek G, Howell SB. Challenges associated with the targeted delivery of gelonin to claudin-expressing cancer cells with the use of activatable cell penetrating peptides to enhance potency. BMC cancer. 2011; 11:61. [PubMed: 21303546]
15. Fawell S, Seery J, Daikh Y, Moore C, Chen LL, Pepinsky B, et al. Tat-mediated delivery of heterologous proteins into cells. Proc Natl Acad Sci USA. 1994; 91(2):664–8. [PubMed: 8290579]
16. Huang Y, Jiang Y, Wang H, Wang J, Shin MC, Byun Y, et al. Curb challenges of the “Trojan Horse” approach: smart strategies in achieving effective yet safe cell-penetrating peptide-based drug delivery. Adv Drug Deliv Rev. 2013; 65:1299–315. [PubMed: 23369828]
17. Jiang T, Olson ES, Nguyen QT, Roy M, Jennings PA, Tsien RY. Tumor imaging by means of proteolytic activation of cell-penetrating peptides. Proc Natl Acad Sci USA. 2004; 101:17867–72. [PubMed: 15601762]
18. Kwon YM, Li YT, Liang JF, Park YJ, Chang LC, Yang VC. PTD-modified ATTEMPTS system for enhanced asparaginase therapy: a proof-of-concept investigation. J Control Release. 2008; 130:252–8. [PubMed: 18652856]
19. Kwon YM, Li Y, Naik S, Liang JF, Huang Y, Park YJ, et al. The ATTEMPTS delivery systems for macromolecular drugs. Expert Opin Drug Del. 2008; 5(11):1255–66.
20. Park YJ, Liang JF, Song H, Li YT, Naik S, Yang VC. ATTEMPTS: a heparin/protamine- based triggered release system for the delivery of enzyme drugs without associated side-effects. Adv Drug Deliv Rev. 2003; 55(2):251–65. [PubMed: 12564979]
21. Shin MC, Zhao J, Zhang J, Huang Y, He H, Wang M, et al. Recombinant TAT-gelonin fusion toxin: Synthesis and characterization of heparin/protamine-regulated cell transduction. J Biomed Mater Res. Apr 15.2014 doi: 10.1002/jbm.a.35188.
22. Stirpe F, Olsnes S, Pihl A. Gelonin, a new inhibitor of protein synthesis, nontoxic to intact cells. Isolation, characterization, and preparation of cytotoxic complexes with concanavalin A. J Biol Chem. 1980; 255(14):6947–53. [PubMed: 7391060]
23. Atkinson SF, Bettinger T, Seymour LW, Behr JP, Ward CM. Conjugation of folate via gelonin carbohydrate residues retains ribosomal-inactivating properties of the toxin and permits targeting to folate receptor positive cells. J Biol Chem. 2001; 276(30):27930–5. [PubMed: 11359781]
24. Shin MC, Zhang J, Min KA, Lee K, Moon C, Balthasar JP, et al. Combination of antibody targeting and PTD-mediated intracellular toxin delivery for colorectal cancer therapy. J Control Release. 2014; 194:197–210. [PubMed: 25204286]
25. Urva SR, Yang VC, Balthasar JP. Physiologically based pharmacokinetic model for T84.66: a monoclonal anti-CEA antibody. J Pharm Sci. 2010; 99:1582–600. [PubMed: 19774657]
26. Yang VC, Linhardt RJ, Bernstein H, Cooney CL, Langer R. Purification and characterization of heparinase from Flavobacterium heparinum. J Biol Chem. 1985; 260:1849–57. [PubMed: 3968088]
27. Bryan JN, Jia F, Mohsin H, Sivaguru G, Miller WH, Anderson CJ, et al. Comparative uptakes and biodistributions of internalizing vs. noninternalizing copper-64 radioimmunoconjugates in cell and animal models of colon cancer. Nucl Med Biol. 2005; 32:851–8. [PubMed: 16253810]
28. Billinton N, Knight AW. Seeing the wood through the trees: a review of techniques for distinguishing green fluorescent protein from endogenous autofluorescence. Anal Biochem. 2001; 291:175–97. [PubMed: 11401292]
29. Zou P, Xu S, Povoski SP, Wang A, Johnson MA, Martin EW Jr. et al. Near-infrared fluorescence labeled anti-TAG-72 monoclonal antibodies for tumor imaging in colorectal cancer xenograft mice. Mol Pharm. 2009; 6(2):428–40. [PubMed: 19718796]
30. Park YJ, Chang LC, Liang JF, Moon C, Chung CP, Yang VC. Nontoxic membrane translocation peptide from protamine, low molecular weight protamine (LMWP), for enhanced intracellular protein delivery: in vitro and in vivo study. FASEB J. 2005; 19:1555–7. [PubMed: 16033808]

31. Park YS, David AE, Huang Y, Park JB, He H, Byun Y, et al. In vivo delivery of cell- permeable antisense hypoxia-inducible factor 1alpha oligonucleotide to adipose tissue reduces adiposity in obese mice. J Control Release. 2012; 161:1–9. [PubMed: 22546680]
32. He H, Sheng J, David AE, Kwon YM, Zhang J, Huang Y, et al. The use of low molecular weight protamine chemical chimera to enhance monomeric insulin intestinal absorption. Biomaterials. 2013; 34:7733–43. [PubMed: 23863452]
33. Brooks H, Lebleu B, Vives E. Tat peptide-mediated cellular delivery: back to basics. Adv Drug Deliv Rev. 2005; 57:559–77. [PubMed: 15722164]
34. He H, Ye J, Liu E, Liang Q, Liu Q, Yang VC. Low molecular weight protamine (LMWP): A nontoxic protamine substitute and an effective cell-penetrating peptide. J Control Release. Jun 3.2014 doi: 10.1016/j.jconrel.2014.05.056.
35. Koren E, Torchilin VP. Cell-penetrating peptides: breaking through to the other side. Trends Mol Med. 2012; 18:385–93. [PubMed: 22682515]
36. Hammarstrom S. The carcinoembryonic antigen (CEA) family: structures, suggested functions and expression in normal and malignant tissues. Semin Cancer Biol. 1999; 9:67–81. [PubMed: 10202129]
37. Gold P, Freedman SO. Specific carcinoembryonic antigens of the human digestive system. J Exp Med. 1965; 122:467–81. [PubMed: 4953873]
38. Neumaier M, Shively L, Chen FS, Gaida FJ, Ilgen C, Paxton RJ, et al. Cloning of the genes for T84.66, an antibody that has a high specificity and affinity for carcinoembryonic antigen, and expression of chimeric human/mouse T84.66 genes in myeloma and Chinese hamster ovary cells. Cancer Res. 1990; 50:2128–34. [PubMed: 2107969]
39. Urva SR, Balthasar JP. Target mediated disposition of T84.66, a monoclonal anti-CEA antibody: application in the detection of colorectal cancer xenografts. MAbs. 2010; 2:67–72. [PubMed: 20081377]
40. Arpicco S, Dosio F, Bolognesi A, Lubelli C, Brusa P, Stella B, et al. Novel poly(ethylene glycol) derivatives for preparation of ribosome-inactivating protein conjugates. Bioconjugate Chem. 2002; 13:757–65.

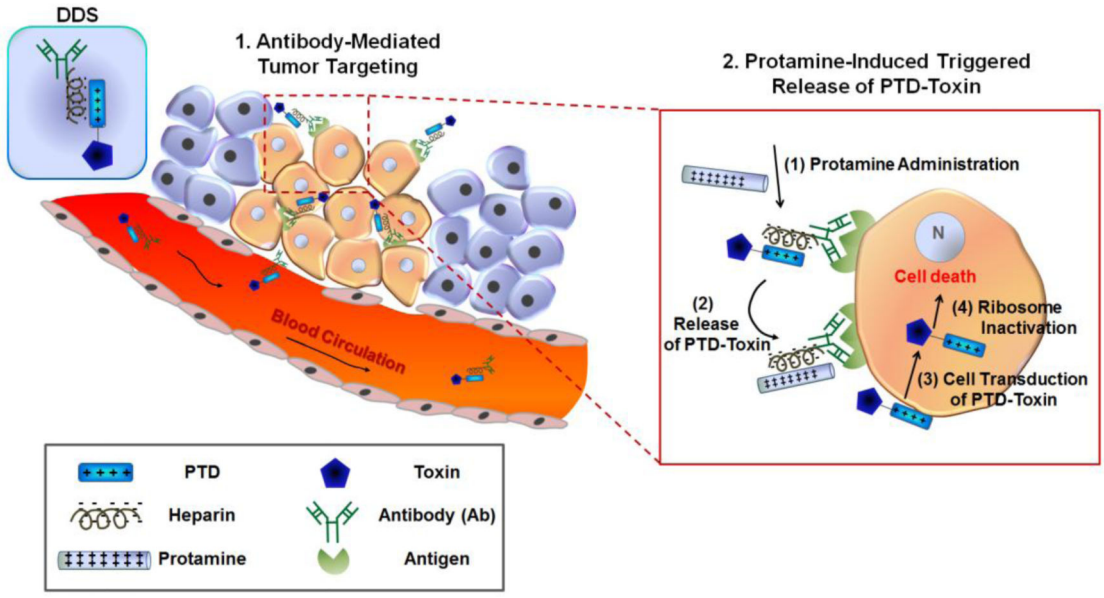

Figure 1.

Scheme of the PTD-modified ATTEMPTS (Antibody Targeted Triggered Electrically Modified Prodrug-Type Strategy) for enhanced toxin therapy for cancer treatment.

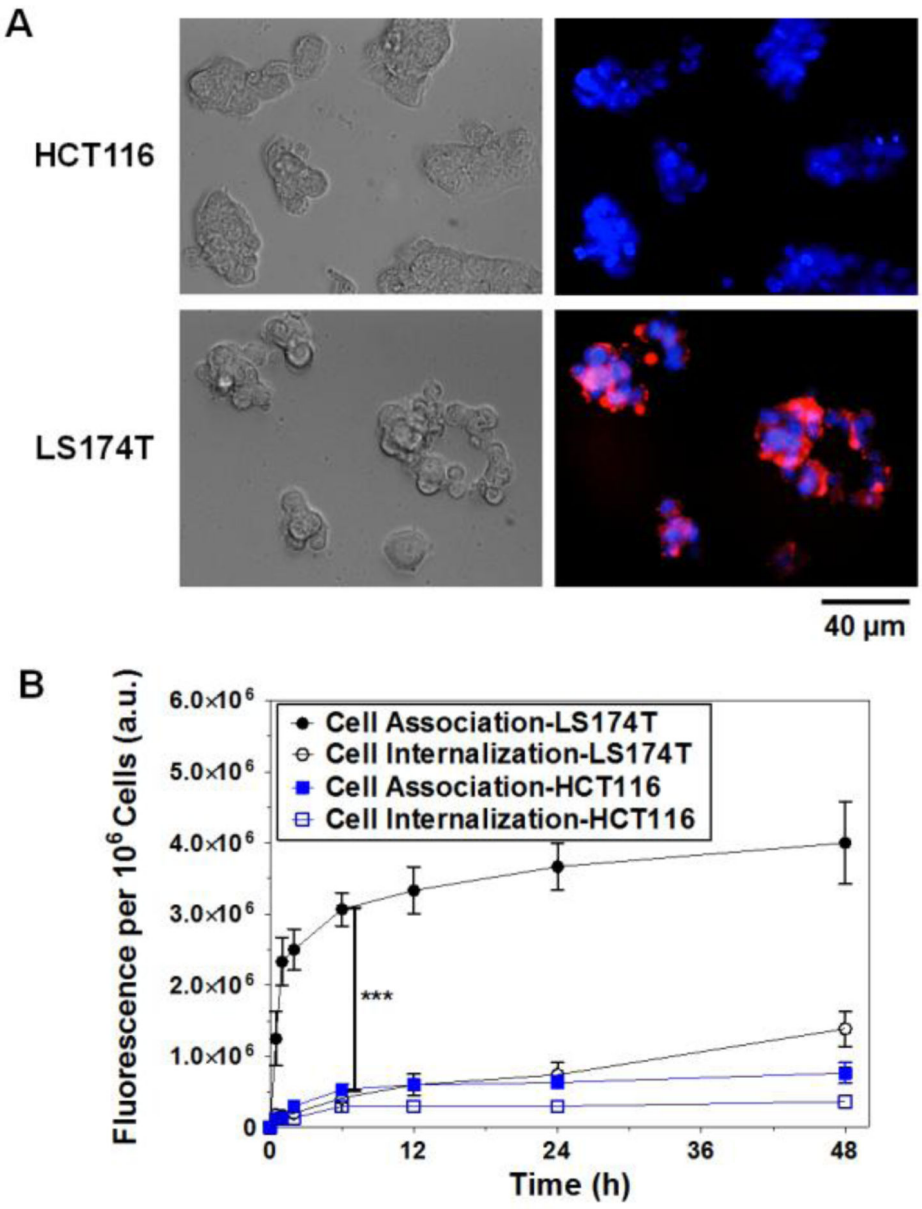

Figure 2.

Cellular analyses of T84.66-Hep binding selectivity and internalization. (A) Brightfield and fluorescence microscopic images of CEA low expression (HCT116) and high expression (LS174T) cells after 2 h incubation with TRITC-labeled T84.66-Hep. The nuclei of the cells were counterstained with Hoechst 33342, and the merged fluorescence images of the cells were generated after fluorescence images were acquired with Hoechst (blue) and TRITC (red) channels. (B) Quantitative analysis of cell association and internalization of T84.66-Hep. HCT116 and LS174T cells were incubated with TRITC-labeled T84.66-Hep at 37°C up to 48 h, and, at intended time points (0, 0.5, 1, 2, 6, 12, 24 and 48 h), the amounts of total associated and internalized T84.66-Hep were quantified by measuring the fluorescence intensity of the cell lysates. ***$P < 0.001$ by Student's t-test. (T84.66-Hep: T84.66-heparin chemical conjugate)

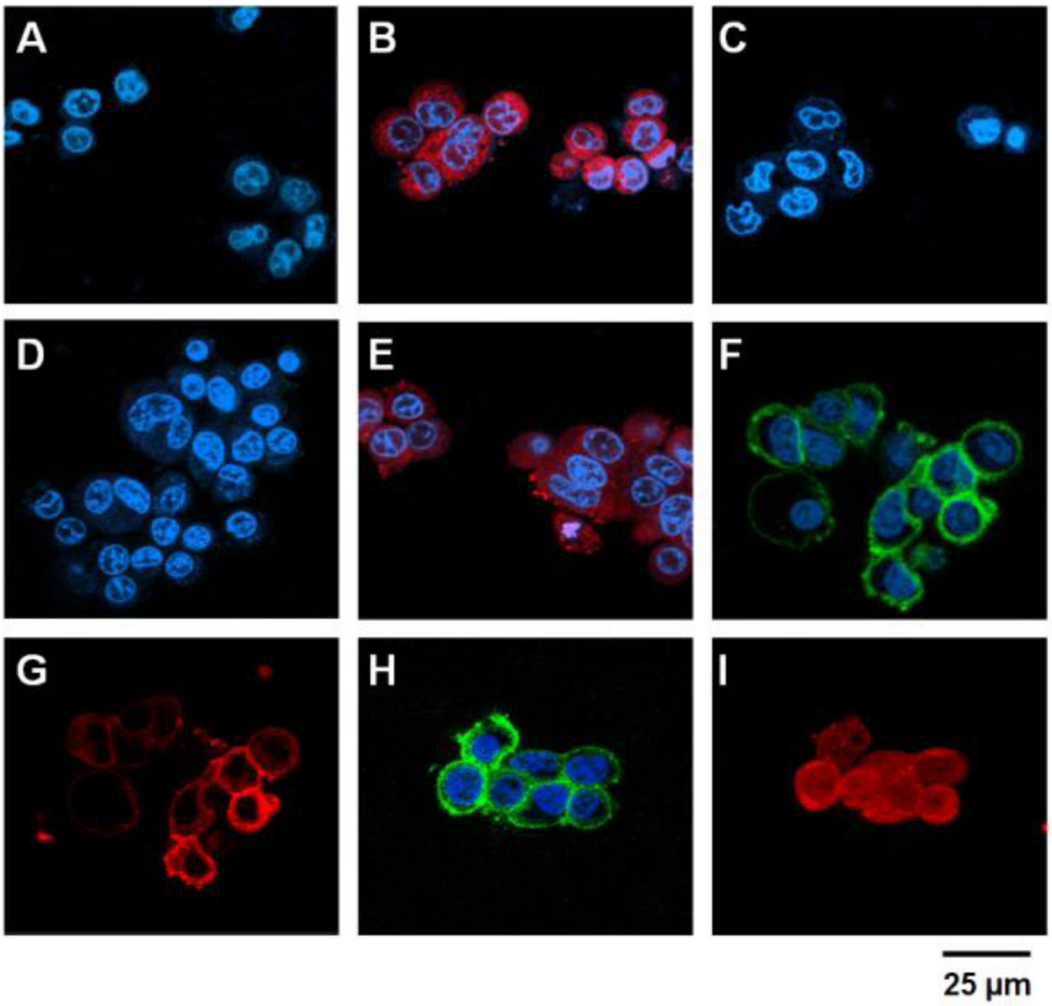

Figure 3.

Confocal microscopic analyses of the PTD-modified ATTEMPTS. HCT116 (A - C) and LS174T cells (D – I) were incubated with either: 1) TRITC-labeled gelonin (A & D), 2) TRITC-labeled TAT-Gel (B & E), 3) TRITC-labeled TAT-Gel/Dylight 488-labeled T84.66-Hep (a.k.a. TAT-Gel/T84.66-Hep) complex (C, F & G) or 4) the TAT-Gel/T84.66-Hep complex with protamine (H & I), and, after counterstaining the nuclei with Hoechst 33342, the fluorescence images of the cells were acquired (Hoechst: blue, TRITC: red and Dylight 488: green). Whereas gelonin entered neither HCT116 (A) nor LS174T (D) cells, a significant uptake of TAT-Gel was observed in both the cell lines (B & E). In a sharp contrast, when the cells were treated with TAT-Gel/T84.66-Hep complex, TAT-Gel was unable to internalize. While TAT-Gel/T84.66-Hep did not bind to HCT116 cells (C), TAT-Gel/T84.66-Hep bound to the LS174T cells (T84.66-Hep: F; TAT-Gel: G), but little internalization. However, to the TAT-Gel/T84.66-Hep-treated LS174T cells, after addition of protamine, TAT-Gel was able to internalize the cells (I), with T84.66-Hep remaining on the cell surface (H). (TAT-Gel: recombinant TAT-gelonin fusion chimera, T84.66-Hep: T84.66-heparin chemical conjugate)

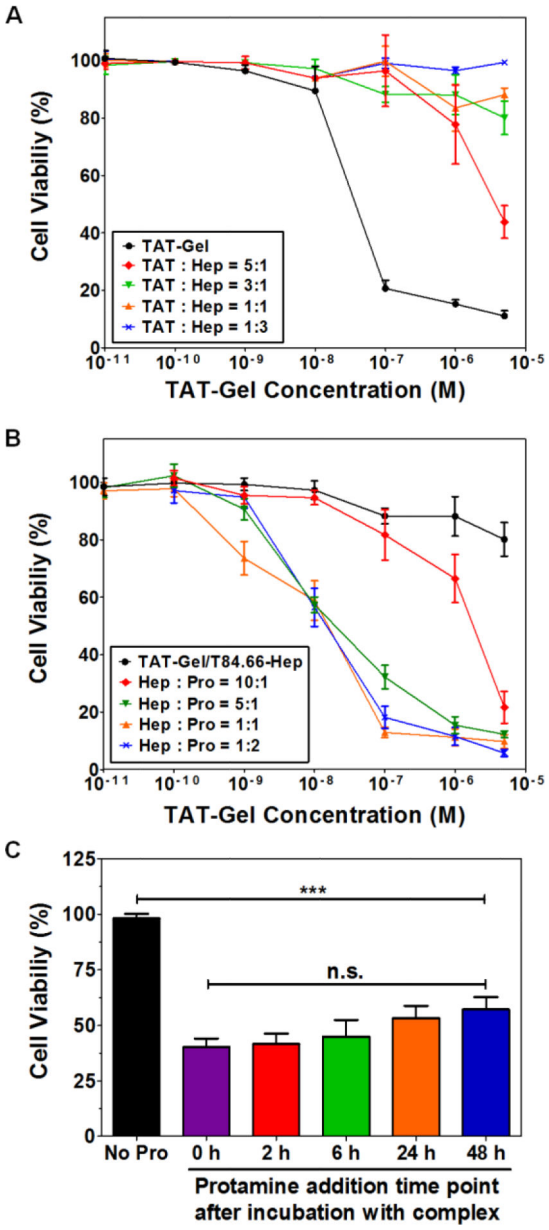

Figure 4.

T84.66-Hep/protamine-mediated modulation of cytotoxicity by TAT-Gel. (A) T84.66-Hep blocking of TAT-Gel cell transduction. When LS174T cells were incubated with TAT-Gel/T84.66-Hep complex, prepared by mixing TAT-Gel with increasing TAT-to-Hep molar ratios (from 5:1 to 1:3) of T84.66-Hep, a significantly reduced cytotoxicity was observed, compared with that of TAT-Gel. (B) Protamine-induced release of TAT-Gel. Addition of protamine to TAT-Gel/T84.66-Hep-treated cells, with increasing Hep-to-Pro molar ratios (from 10:1 to 1:2), cytotoxicity effects were significantly augmented. At above 5:1 molar ratio, the anti-cancer effect (IC_{50}) was similar to that induced by TAT-Gel alone. (C) Time dependency of the protamine addition time on effects of protamine-triggered release. Cells were incubated with TAT-Gel/T84.66-Hep for 6 h, and, after wash, at intended time points (0, 2, 6, 24 and 48 h), protamine (Hep : Pro molar ratio of 1:2) was added to the wells, and

the cells were incubated with protamine further up to total 72 h. ***$P < 0.001$ and *n.s.*: not significant by 1-way ANOVA (Tukey's multiple comparison test as the post hoc test). (TAT-Gel: recombinant TAT-gelonin fusion chimera, T84.66-Hep: T84.66-heparin chemical conjugate, Hep: heparin, Pro: protamine)

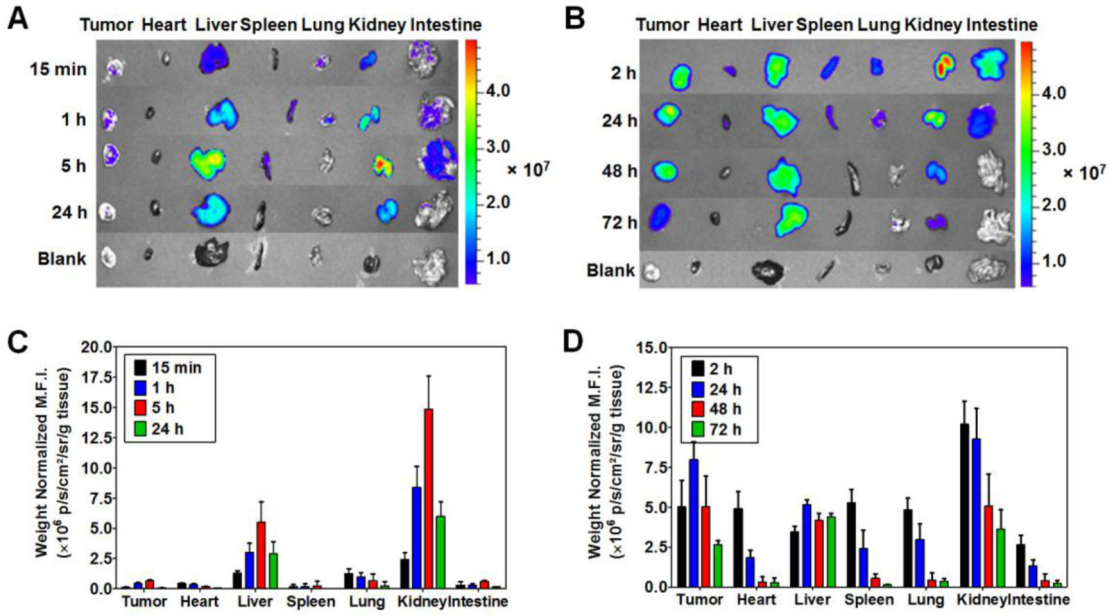

Figure 5.

Biodistribution of TAT-Gel. LS174T *s.c.* xenograft tumor bearing mice were administered with either (A) Dylight 775-B4 labeled-TAT-Gel (a.k.a. TAT-Gel-B4) or (B) TAT-Gel-B4/T84.66-Hep *via* tail vein injection, and at intended time points, the mice were euthanized and the major organs were harvested and imaged by using IVIS® spectrum imaging system (Xenogen, Alameda, CA). Administration of TAT-Gel/T84.66-Hep resulted in prolonged blood circulation of TAT-Gel; as evidenced from the fluorescence intensity observed in the heart up to 24 h, and a significantly enhanced (43-fold) tumor exposure. (TAT-Gel: recombinant TAT-gelonin fusion chimera, T84.66-Hep: T84.66-heparin chemical conjugate)

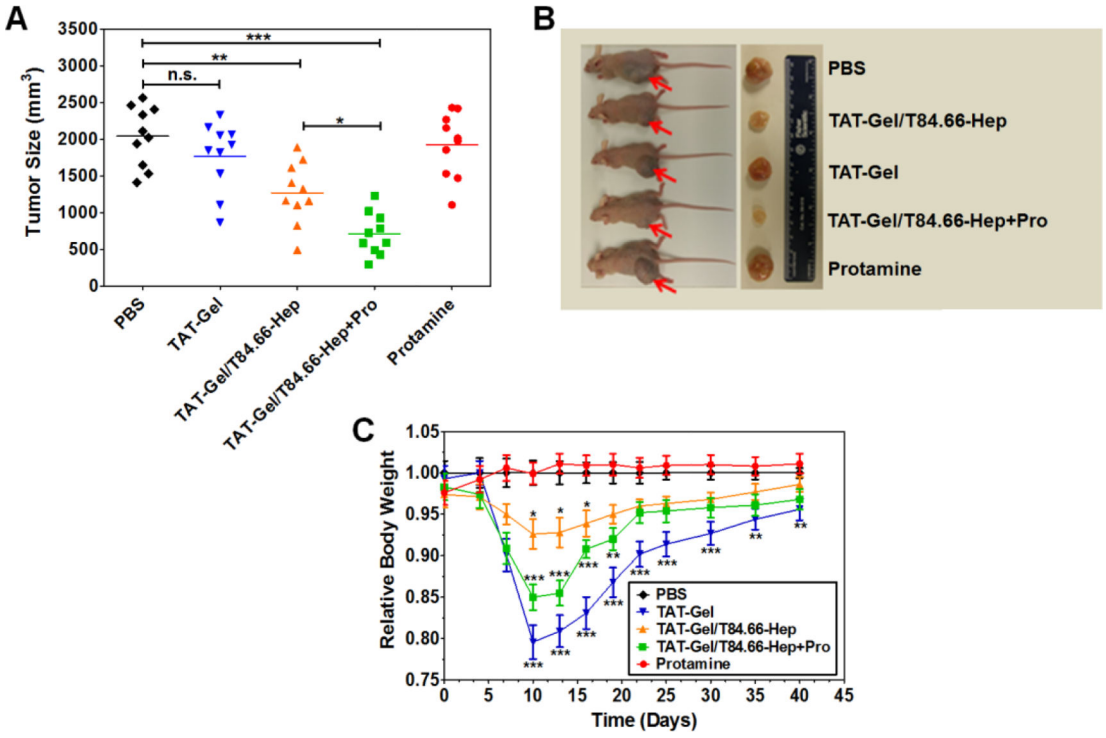

Figure 6.

In vivo proof-of-concept efficacy study for assessment of the feasibility of PTD-modified ATTEMPTS using LS174T xenograft tumor bearing mice. (A) Tumor volumes (mm^3) at day 40 (40 days after tumor implantation). At day 3, mice were divided into 5 groups (N = 10) and treated with either: 1) PBS, 2) TAT-Gel, 3) TAT-Gel/T84.66-Hep, 4) "TAT-Gel/T84.66-Hep+Pro" or 5) protamine (a.k.a. Pro) for three times (at day 3, 6 and 9) *via* tail vein injection. (B) Representative mice and tumor images at day 40. (C) Relative average body weight change (%) of mice during efficacy study. "TAT-Gel/T84.66-Hep+Pro" treatment exerted significantly enhanced therapeutic effects (*$P < 0.05$), compared with TAT-Gel/T84.66-Hep treatment, yet induced higher toxicity. *$P < 0.05$, **$P < 0.01$ and ***$P < 0.001$ by 1-way ANOVA (Tukey's multiple comparison test as the post hoc test). (TAT-Gel: recombinant TAT-gelonin fusion chimera, T84.66-Hep: T84.66-heparin chemical conjugate, TAT-Gel/T84.66-Hep+Pro": treatment with TAT-Gel/T84.66-Hep complex with protamine)

Table 1

T84.66-Hep and protamine mediated modulation of cytotoxicity induced by TAT-Gel

Test Compound	TAT : Hep molar ratio	IC_{50} [a], nM	Test Compound	Hep : Pro molar ratio	IC_{50} [a], nM
TAT-Gel		29.2 ± 7.9	Protamine		> 5000***
TAT-Gel/T84.66-Hep	5:1	2410 ± 890**	"TAT-Gel/T84.66-Hep+Pro"	10:1	1830 ± 700*
	3:1	> 5000***		5:1	23.4 ± 4.2
	1:1	> 5000***		1:1	17.4 ± 3.1
	1:3	> 5000***		1:2	15.6 ± 3.4
T84.66-Hep		> 5000***	"TAT-Gel+Pro"		19.6 ± 4.3

[a] IC_{50} values were calculated by nonlinear regression using Prism software (GraphPad). For all experiments, N = 3. Statistical analysis results are shown in comparison with TAT-Gel data.

* P < 0.05

** P < 0. 01

*** *P < 0.001* by 1-way ANOVA (Tukey's multiple comparison test as the post hoc test). (TAT-Gel: recombinant TAT-gelonin fusion chimera, T84.66-Hep: T84.66-heparin chemical conjugate)